ACS Macro Letters

Letter

pubs.acs.org/macroletters

Super Stretchy Polymer Multilayer Thin Film with High Gas Barrier

Fangming Xiang,[†] Sarah M. Ward,[‡] Tara M. Givens,[†] and Jaime C. Grunlan*[,†,‡]

[†]Department of Mechanical Engineering and [‡]Department of Chemistry, Texas A&M University, College Station, Texas 77843, United States

Supporting Information

ABSTRACT: Unlike ionically bonded or clay-loaded gas barrier thin films, which easily crack when moderately stretched, hydrogen-bonded poly(acrylic acid) (PAA)/poly(ethylene oxide) (PEO) multilayer thin films remain crack-free. Even after 100% strain, these nanocoatings provide more than a 5× reduction in oxygen transmission rate. This study shows that the lowest modulus PAA/PEO thin film is obtained at pH 3, but maintains a high barrier. A total of 20 PAA/PEO bilayers (367 nm thick) on 1.58 mm rubber reduced the oxygen transmission rate by 1 order of magnitude. Stretching from 25−100% caused plastic deformation and reduced gas barrier, but the oxygen transmission rate remained at least 5× lower than the uncoated rubber. The ability to prevent cracking and preserve the gas barrier up to 100% strain provides a tremendous opportunity for reducing weight and improving the barrier of elastomeric materials.

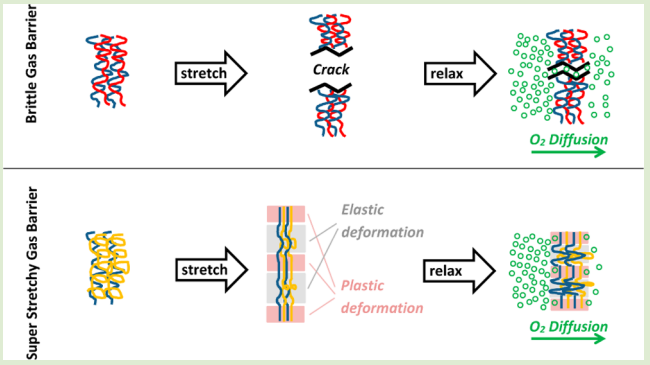

Layer by layer (LbL) thin film assemblies are well-known for their ability to provide a high barrier to gases,[1−6] but they are typically very stiff (as high as 106 GPa),[2,7,8] making them unsuitable for high strain applications. For example, extensive mud-cracking was observed on the poststretched surface of a 125 nm thick polyethylenimine/montmorillonite clay assembly, whose oxygen transmission rate (OTR) increased more than 40x after 10% stretching.[9] The brittleness of the existing gas barrier thin films originates from their composition and bonding type. LbL films assembled with clay are highly brittle due to the inherent rigidity of clay platelets[10] and clay concentrations (exceeding 70 wt %).[7] Even without clay present, multilayer thin films assembled using electrostatic bonding are also very stiff, because movement of polymer chains is restricted by the strong and numerous ionic cross-links between them.[2,11] Hydrogen bonding features smaller bond strength and looser cross-linking density,[12−15] relative to ionic bonding, allowing for easier polymer chain mobility and enhanced thin film ductility. On this basis, it can be concluded that LbL films without rigid nanoparticles (e.g., clay) and electrostatic bonding are more likely to be stretchable. It is for this reason that thin films assembled using poly(acrylic acid) [PAA] and poly(ethylene oxide) [PEO] were studied in an effort to produce a stretchy gas barrier nanocoating for elastomeric substrates.

Multilayer thin films assembled with H-bond donating PAA and H-bond accepting PEO are already known to exhibit excellent ductility. It was reported that a 100 bilayer (BL) free-standing PAA/PEO film was stretched to five times its original length before breaking.[13] Mechanical testing of PAA/PEO thin films, assembled at varying pH, reveals that the softest film can be obtained at pH 3 (referred to as PAA_3/PEO_3). The 20 BL PAA_3/PEO_3 assembly not only exhibits reasonable gas barrier when unstretched, but is capable of preserving much of its gas barrier even after 100% strain. This study marks the first report of a super stretchy gas barrier that can be used in applications requiring a gas barrier coating able to withstand large-strain (>25%), such as inflatable elastomers used in tires and seals.

Figure 1a shows how the glass transition temperature (T_g) of 100 BL free-standing PAA/PEO assemblies decreases with increasing deposition pH due to less carboxylic acid dimer and more deprotonated acid groups (detailed information about film buildup and characterization is provided in the Experimental Section in the Supporting Information).[12,16] The DSC curves of all samples can be found in the Supporting Information (Figure S1). This change in T_g results in a corresponding change in room temperature elastic modulus of 40 BL PAA/PEO thin films, also shown in Figure 1a, which was measured using an atomic force microscope (AFM). In this experiment, a standard AFM probe was used to obtain a force−distance curve.[17,18] The elastic modulus was calculated using the retraction curve near the peak force, in conjunction with the Hertz model. A remarkable drop in modulus is observed when the glass transition temperature becomes lower than the testing temperature (23 °C). The softest PAA/PEO thin films, obtained at pH 3, were used in the following gas barrier and strain testing to minimize the possibility of cracking during stretching. Similar to previous findings,[16] the thickness of PAA/

Received: August 27, 2014
Accepted: October 1, 2014
Published: October 6, 2014

   dx.doi.org/10.1021/mz500532q | ACS Macro Lett. 2014, 3, 1055−1058

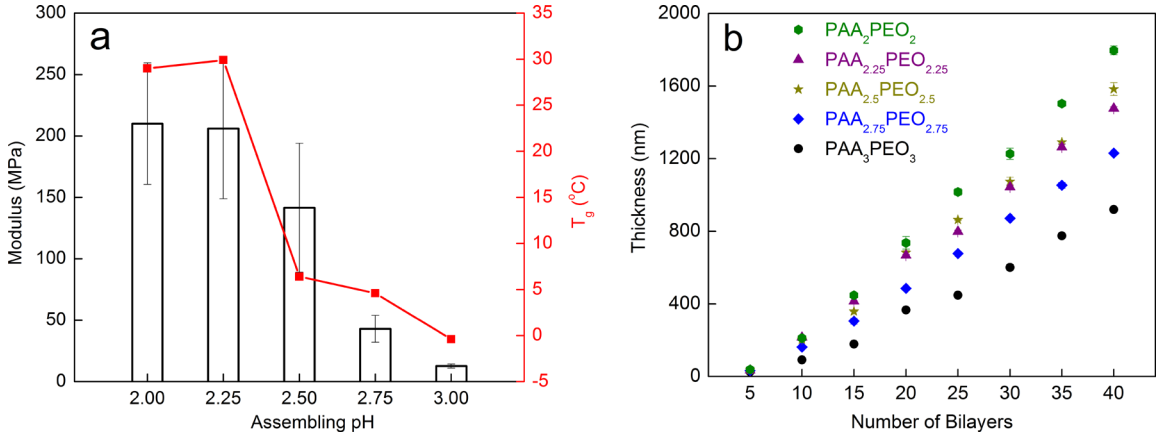

Figure 1. Elastic modulus and glass transition temperature as a function of deposition pH for PAA/PEO multilayer thin films (a). Thickness as a function of PAA/PEO bilayers deposited at varying pH (b).

PEO assemblies is found to decrease with increasing pH, as shown in Figure 1b. The PAA/PEO assemblies investigated here are thinner than those reported earlier due to shorter deposition time used in this study (1 min instead of 10 min).[16] PAA/PEO thin films assembled beyond pH 3 were not investigated because film growth becomes very inconsistent.[13]

Polymer thin films with high gas barrier usually have high cohesive energy density,[19] which prevents gas molecules from moving aside polymer chains.[20,21] Despite being weaker than electrostatic bonding, hydrogen-bonding between polymer chains imparts reasonable gas barrier to the assembly. As shown in Figure 2, a 367 nm thick 20 BL PAA_3/PEO_3

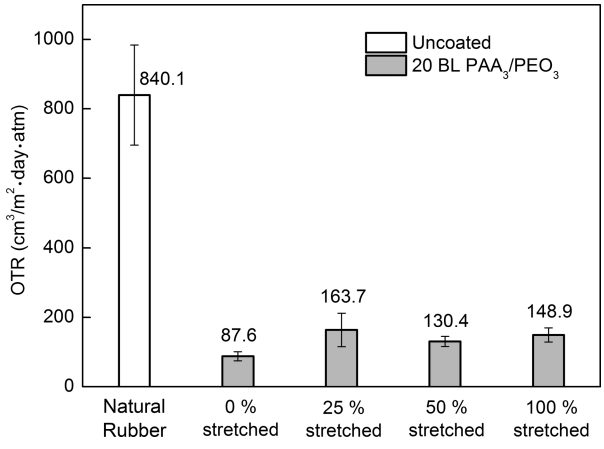

Figure 2. Oxygen transmission rate of 1.58 mm natural rubber sheet, coated with 20 BL PAA_3/PEO_3, stretched to varying extents.

nanocoating can reduce the OTR of 1.58 mm thick natural rubber by 1 order of magnitude (from 840.1 to 87.6 $cm^3/(m^2$·day·atm)). Although stretching reduces gas barrier in general, increasing the strain level does not lead to larger OTR and barrier remains a factor of 5 better than uncoated rubber at 100% strain.

In an effort to better understand the influence of stretching on gas barrier, surface morphology of coated samples before and after stretching was imaged with a field emission scanning electron microscope (FESEM). As shown in Figure 3a, the 20 BL PAA_3/PEO_3 nanocoating is quite smooth at 0% strain. Stretching to 25 and 50% strain has little influence on surface morphology, except for the formation of a few shallow lines

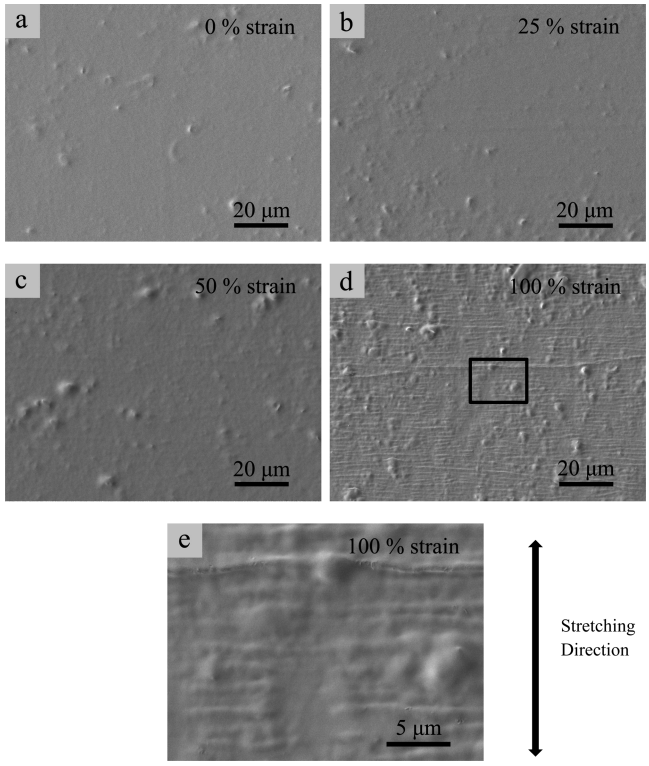

Figure 3. FESEM surface images of 20 BL PAA_3/PEO_3 coated rubber after 0 (a), 25 (b), 50 (c), and 100% (d, e) strain [(e) is the magnified image of the area indicated in (d)].

perpendicular to the stretch direction. These lines become more dense and pronounced when the strain level reaches 100%. When observed at a higher magnification (Figure 3e), these lines appear to be creases rather than cracks.

The influence of stretching on structure and morphology can be correlated with the gas barrier of the PAA_3/PEO_3 assembly using the mechanism proposed in Figure 4. It was reported that $PAA_{2.5}/PEO_{2.5}$ transformed from elastic to plastic deformation around 10% strain.[13] Since both $PAA_{2.5}/PEO_{2.5}$ and PAA_3/PEO_3 exist in their rubbery state under ambient conditions (23 °C, 45% relative humidity (RH)), it is reasonable to assume that both would exhibit similar tensile behavior and become plastically deformed at 25%, as shown schematically in Figure 4b. Although plastic deformation has little influence on

dx.doi.org/10.1021/mz500532q | ACS Macro Lett. 2014, 3, 1055−1058

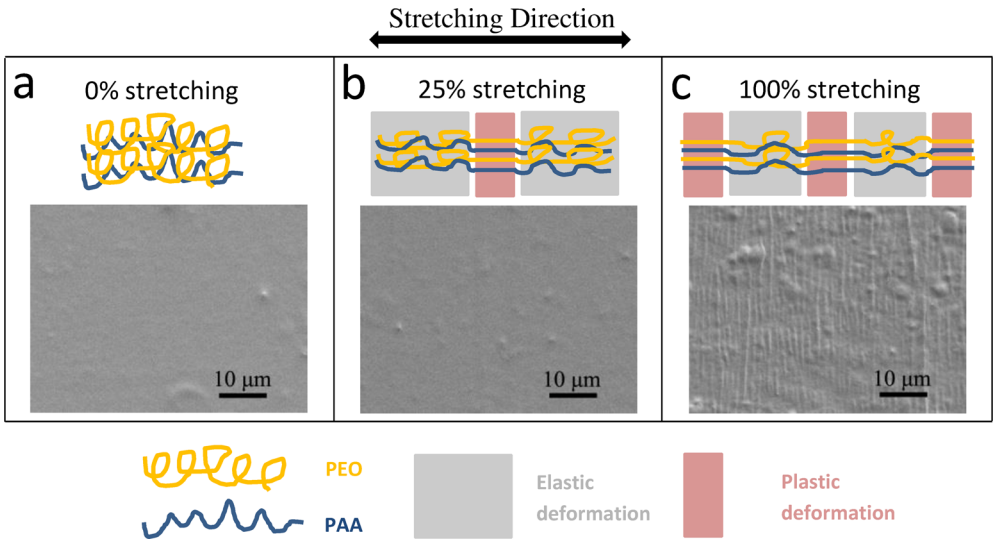

Figure 4. Schematic showing the influence of different strain levels 0 (a), 25 (b), and 100% (c) on structure and morphology of PAA_3/PEO_3 assembly (FESEM surface images are below each schematic).

morphology, it leads to reduced gas barrier, possibly due to thinning of film. Figure 4c shows that increasing the strain level to 100% induces plastic deformation at multiple locations. The plastically extended parts of the film fold up after being released, resulting in creases perpendicular to the stretching direction. It is interesting to note that although a remarkable change in surface morphology can be observed after 100% stretching, the OTR of this sample is nearly identical to films tested with lower strain levels. It is believed that smaller, less visible plastic deformation generated at lower strain levels (25 and 50%) reduce the gas barrier of the 20 BL PAA_3/PEO_3 thin film. It is a bit surprising that larger and more visible plastic deformations generated at 100% strain did not further reduce gas barrier. As can be seen in Figure 2, the oxygen transmission rate of 25, 50, and 100% strained samples are statistically the same. This result suggests that plastically deformed films have similar gas barrier, regardless of the extent of the damage. There would likely be another drop in barrier upon rupture of the film, but this did not occur up to 100% strain.

In conclusion, by assembling hydrogen-bond donating PAA with hydrogen-bond accepting PEO, ductile thin film assemblies can be obtained due to the absence of strong electrostatic bonding. The softest PAA/PEO assembly is obtained at pH 3, and a 367 nm thick 20 BL PAA_3/PEO_3 nanocoating reduces the oxygen transmission rate of 1.58 mm thick natural rubber by 1 order of magnitude when unstretched. Thanks to its excellent ductility, plastic deformation of the PAA_3/PEO_3 assembly is distributed to multiple locations and kept at a relatively low level to prevent strain-induced cracking. It is for this reason that the negative impact of plastic deformation on gas barrier can be minimized, enabling this thin film to maintain a 5× reduction in rubber OTR even after 100% stretching. It is possible that the gas barrier of PAA_3/PEO_3 may be reduced after cyclic loading due to accumulated plastic deformation. LbL assembly with larger elastic deformation capability would alleviate this potential problem. Lower T_g assemblies are currently being developed for this purpose. These unique stretchy barriers offer the opportunity for lightweight, energy-saving rubber that can maintain relative high gas pressure.

■ ASSOCIATED CONTENT

Ⓢ Supporting Information

Experimental information and DSC curves. This material is available free of charge via the Internet at http://pubs.acs.org.

■ AUTHOR INFORMATION

Corresponding Author

*Phone: 979-845-3027. E-mail: jgrunlan@tamu.edu.

Notes

The authors declare no competing financial interest.

■ ACKNOWLEDGMENTS

The authors acknowledge the Texas A&M Engineering Experiment Station (TEES), and the Texas A&M University Materials Characterization Facility (MCF) for infrastructural support of this research. Dr. Wilson Serem, at the MCF, is especially thanked for his help with AFM.

■ REFERENCES

(1) Priolo, M. A.; Gamboa, D.; Holder, K. M.; Grunlan, J. C. *Nano Lett.* **2010**, *10*, 4970−4974.
(2) Yang, Y. H.; Haile, M.; Park, Y. T.; Malek, F. A.; Grunlan, J. C. *Macromolecules* **2011**, *44*, 1450−1459.
(3) Stevens, B.; Dessiatova, E.; Hagen, D. A.; Todd, A. D.; Bielawski, C. W.; Grunlan, J. C. *ACS Appl. Mater. Interfaces* **2014**, *6*, 9942−9945.
(4) Svagan, A. J.; Åkesson, A.; Cárdenas, M.; Bulut, S.; Knudsen, J. C.; Risbo, J.; Plackett, D. *Biomacromolecules* **2012**, *13*, 397−405.
(5) Aulin, C.; Karabulut, E.; Tran, A.; Wågberg, L.; Lindström, T. *ACS Appl. Mater. Interfaces* **2013**, *5*, 7352−7359.
(6) Chen, J.-T.; Fu, Y.-J.; An, Q.-F.; Lo, S.-C.; Huang, S.-H.; Hung, W.-S.; Hu, C.-C.; Lee, K.-R.; Lai, J.-Y. *Nanoscale* **2013**, *5*, 9081−9088.
(7) Priolo, M. A.; Gamboa, D.; Grunlan, J. C. *ACS Appl. Mater. Interfaces* **2010**, *2*, 312−320.
(8) Podsiadlo, P.; Kaushik, A. K.; Arruda, E. M.; Waas, A. M.; Shim, B. S.; Xu, J.; Nandivada, H.; Pumplin, B. G.; Lahann, J.; Ramamoorthy, A.; Kotov, N. A. *Science* **2007**, *318*, 80−83.
(9) Holder, K. M.; Spears, B. R.; Huff, M. E.; Priolo, M. A.; Harth, E.; Grunlan, J. C. *Macromol. Rapid Commun.* **2014**, *35*, 960−964.
(10) Chen, B.; Evans, J. R. *Scr. Mater.* **2006**, *54*, 1581−1585.
(11) Zacharia, N. S.; Modestino, M.; Hammond, P. T. *Macromolecules* **2007**, *40*, 9523−9528.

(12) Lutkenhaus, J. L.; McEnnis, K.; Hammond, P. T. *Macromolecules* **2007**, *40*, 8367−8373.
(13) Lutkenhaus, J. L.; Hrabak, K. D.; McEnnis, K.; Hammond, P. T. *J. Am. Chem. Soc.* **2005**, *127*, 17228−17234.
(14) Sukhishvili, S. A.; Granick, S. *Macromolecules* **2002**, *35*, 301−310.
(15) Kharlampieva, E.; Sukhishvili, S. A. *J. Macromol. Sci., Polym. Rev.* **2006**, *46*, 377−395.
(16) DeLongchamp, D. M.; Hammond, P. T. *Langmuir* **2004**, *20*, 5403−5411.
(17) Adamcik, J.; Lara, C.; Usov, I.; Jeong, J. S.; Ruggeri, F. S.; Dietler, G.; Lashuel, H. A.; Hamley, I. W.; Mezzenga, R. *Nanoscale* **2012**, *4*, 4426−4429.
(18) Pittenger, B.; Erina, N.; Su, C. *Application Note Veeco Instruments Inc.*, 2010, http://www.veeco.com/pdfs/appnotes/Quantitative-Mechanical-Property-Mapping-at-the-Nanoscale-with-PeakForce-QNM-AN128-LoRes.pdf.
(19) Lagaron, J.; Catalá, R.; Gavara, R. *Mater. Sci. Technol.* **2004**, *20*, 1−7.
(20) Kochumalayil, J. J.; Berglund, L. A. *Green Chem.* **2014**, *16*, 1904−1910.
(21) Lagaron, J. M.; Powell, A. K.; Bonner, G. *Polym. Test.* **2001**, *20*, 569−577.